Improvement of inclined anchors pullout capacity in geogrid-reinforced sand

Sougata Mukherjee[1*], and *G L Sivakumar* Babu[2]

[1]Research scholar, Department of Civil Engineering, Indian Institute of Science, Bengaluru, 560012, India
[2]Professor, Department of Civil Engineering, Indian Institute of Science, Bengaluru, 560012, India

Abstract. A three-dimensional numerical analysis of inclined anchors embedded in unreinforced and geogrid-reinforced sand is presented in this paper. The pullout forces and breakout factors are compared for the unreinforced and reinforced cases. The pullout capacity increased when placed below a layer of geogrid reinforcement. The influence of several other parameters, such as geogrid stiffness, inclination angle, soil friction angle, and embedment ratio, are investigated and reported in this study. Finally, a comparison between pile and anchor foundation is shown for a transmission tower subjected to lateral wind force.

1 Introduction

Anchor plates are frequently used below structures where pullout forces generated from wind, earthquake, and buoyant forces are anticipated at the foundation levels during the service period. The use of inclined anchors in combination with shallow foundations can be found in transmission towers [1]. The pullout capacity of inclined anchors in sand is well investigated in the literature [2–4]. The influence of geogrid reinforcement on the pullout capacity of anchor has been studied previously [5,6] using small-scale laboratory experiments. The results indicate that the anchor pullout capacity improves significantly in presence of geogrid. However, the small-scale results are prone to scale effects. Also, only a limited number of test results corresponding to some specific cases have been reported in the literature. This paper presents a large-scale numerical analysis of inclined square anchors in geogrid reinforced sand using three-dimensional numerical analysis. The influence of several parameters, namely geogrid stiffness, Inclination angle, friction angle, and the embedment ratio of the anchor plate, are analyzed in this paper. Finally, the application and benefits of reinforced anchors are demonstrated with the help of an illustrative example of a transmission tower subjected to lateral wind loads.

2 Numerical model details and validation

The three-dimensional finite difference computer program FLAC 3D (Fast Lagrangian Analysis of Continua in 3D) has been used for the numerical simulation of geogrid reinforced

* Corresponding author: msougata@iisc.ac.in

anchor. The geometry of the anchor plate and reinforcement and other parameters are presented in Fig. 1. An anchor plate of width B inclined at an inclination angle of α is buried at a depth of H under a reinforcement layer of width b. The sand in the numerical model is simulated using the Mohr-Coulomb constitute model, and the anchor plate was simulated using the Liner structural element. The Geogrid structural element was used to model the reinforcement layer placed over the anchor plate. The numerical model and the grid are shown in Fig. 2.

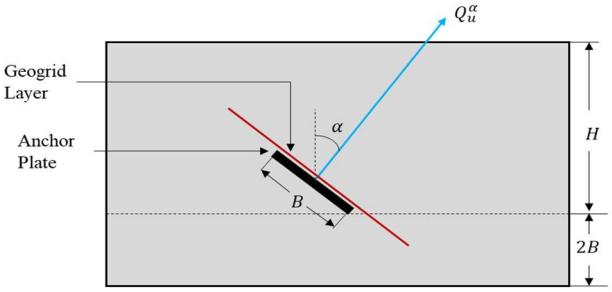

Fig. 1. Schematic layout of anchor geometry

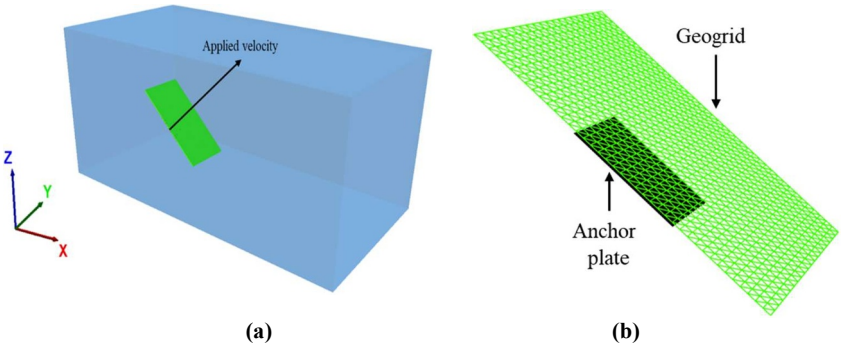

Fig. 2. Numerical model from FLAC 3D (a) numerical model, (b) anchor and reinforcement

Table 1. Soil and geogrid properties used by Mukherjee et al. [5]

Parameters	Values
Soil properties	
Unit Weight at 70% RD, $\boldsymbol{\gamma}$ (kN/m^3)	16.6
Friction Angle ($\boldsymbol{\phi}$) at 70% RD	38˚
Cohesion, c (kPa)	0
Bulk Modulus, $\boldsymbol{K}$ (MPa)	11.83
Shear Modulus, $\boldsymbol{G}$ (MPa)	5.46
Geogrid properties	
Thickness (mm)	1
Mesh opening size (mm×mm)	38×38
Tensile strength at 2% strain (kN/m)	7
Tensile stiffness, $\boldsymbol{J}$ (kN/m)	350
Interface friction angle, $\boldsymbol{\phi_i}$ (◦)	19
Interface cohesion, $\mathbf{c_i}$(MPa)	0

The numerical model is validated by simulating the experimental results reported by Mukherjee et al. [5]. The authors conducted experiments on inclined anchors in unreinforced and geogrid-reinforced sand. The properties of sand and geogrid used in the experiments are summarized in Table 1. The same properties were used to simulate the test conditions for α=30°, 45° and 60° at an embedment ratio of H/B=3. The comparison between the numerical and experimental results is plotted in Fig. 3.

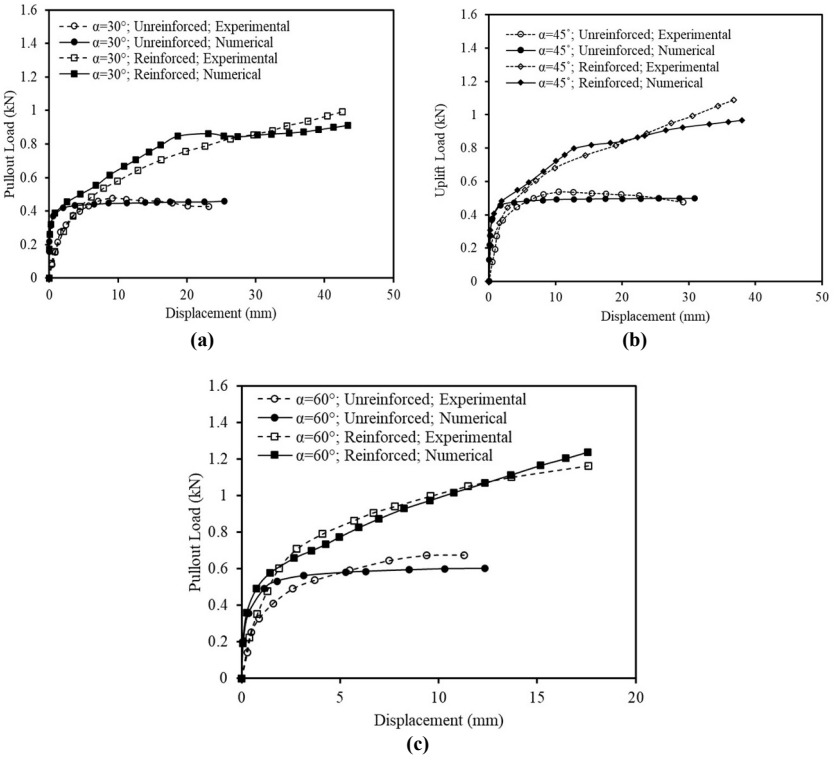

Fig. 3. Validation of numerical model (a) α=30°; (b) α=45°; (c) α=60°.

Results from numerical analysis

Numerical simulations were conducted in FLAC 3D using three types of sand properties listed in Table 2. A square anchor of width B=0.5 m was used in the simulations. A constant width of the geogrid b=3B was used in the analyses. The behavior of unreinforced and reinforced anchor's pullout capacity was investigated at three different inclination angles, α=30°, 45°, and 60°. The reinforcement properties used in the simulations are the same as those mentioned in Table 1. As the anchors in reinforced sand require large displacement, beyond the foundation's allowable displacement limit, for ultimate failure, an axial pullout displacement of 20% was allowed in the numerical simulations

The comparison of pullout load versus percentage displacement plots between unreinforced and reinforced anchors is shown in Fig. 4. The results clearly show the improvement in the pullout capacity of the anchor in reinforced sand. Besides, it can be seen that the unreinforced

anchors reached their peak pullout capacity within the 20% displacement. However, no such peak was observed in the case of reinforced anchors. For example, the anchor placed in unreinforced sand of ϕ=35° reached the maximum pullout load within 10% displacement. On the other hand, the pullout capacity of the reinforcement anchor increased up to the end of 20% displacement. There are two primary reasons behind this increase in the reinforced anchor's pullout capacity. One is the distribution of the uplift pressure over a wider region in the reinforced soil mass by the geogrid reinforcement layer. Another is the mobilization of tensile forces in the reinforcement and the interlocking between the soil and geogrid, thereby increasing the anchor pullout capacity.

Table 2. Soil properties used in the numerical study

Friction angle ϕ (°)	Dilation angle ψ (°)	Cohesion (kPa)	Unit weight γ (kN/m^3)	Elastic modulus, E_s (MPa)	Poisson's ratio μ
35	5	0.5	16.5	30	0.3
40	10	0.5	17.1	45	0.3
45	15	0.5	17.9	60	0.3

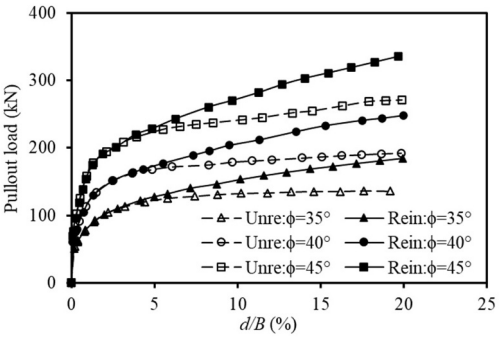

Fig. 4. Pullout load vs. percentage displacement for unreinforced and reinforced anchor for α=45° and H/B=4

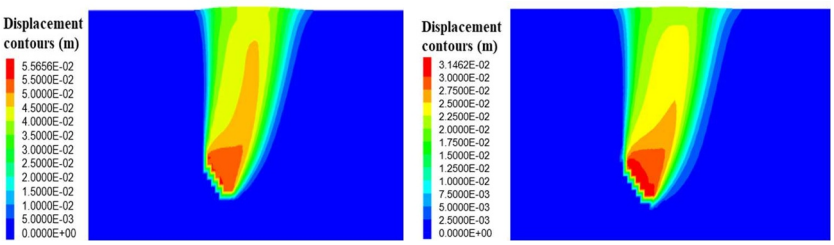

Fig. 5. Displacement contours at H/B=4, α=45°, ϕ=40° for pullout load of 180 kN **(a)** unreinforced anchor **(b)** reinforced anchor

The displacement contour plots for a pullout load of 180 kN for the case of α=45°, ϕ= 40°, and H/B=4 are shown in Fig. 5. The maximum displacement of the reinforced anchor is reduced by 43.5% compared to the unreinforced case. The maximum tensile forces mobilized in the reinforcement layer are plotted in Fig. 6 for α=45°. The results indicate that the tensile

force increases with the embedment ratio. However, the rate of increase in the tensile force decreases with an increase in the embedment ratio.

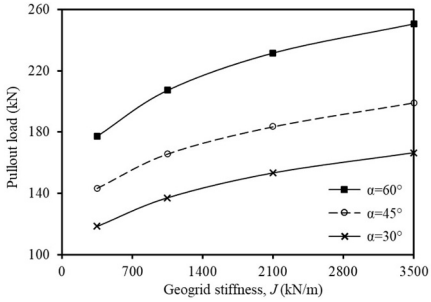

Fig. 6. Mobilized tensile force in the reinforcement for α=45°.

The influence of the geogrid stiffness on the pullout capacity of inclined reinforced anchors is investigated by varying the geogrid stiffness from 350 kN/m to 3500 kN/m. The variation of the pullout load with geogrid stiffness is shown in Fig. 6. The pullout load increased with an increase in the geogrid stiffness due to the higher tensile force mobilized in the reinforcement.

The variation of the pullout capacity with the anchor inclination angle (α) is shown in Fig. 7. The pullout capacity increases with the inclination angle. As the inclination angle increases, the passive failure zone in front of the anchor plate extends in the soil mass, thereby involving a greater soil mass in the failure zone. The extended failure surface also mobilizes higher shear strength along it. These two are the primary reasons behind the increase in the pullout capacity of the inclined anchor with an increase in α.

The influence of the embedment ratio on the anchor pullout capacity is shown in Fig. 8. The anchor capacity is expressed in terms of the non-dimensional breakout factor, defined as $F_q = Q_u/(\gamma AH)$, where γ is the unit weight of soil, A is the anchor surface area. H is the embedment depth of the anchor plate. The embedment depth, beyond which the breakout factor ceases to increase, is the critical depth. An anchor placed below the critical depth shows shallow anchor behavior in which the failure surface reaches the ground surface. In comparison, anchors placed below the critical depth exhibit deep anchor failure. The critical depth was found to be influenced by the relative density of the sand, as indicated by Fig. 8.

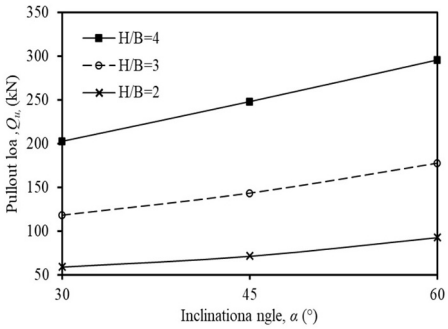

Fig. 7. Variation of pullout load with inclination angle

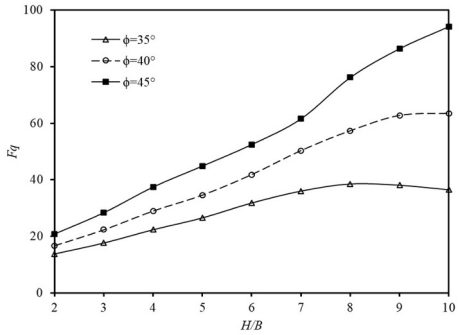

Fig. 8. Variation of breakout factor with embedment ratio.

The anchor reaches its critical depth at H/B=10 in the case of ϕ=35°. However, no such critical depth was observed in the case of very dense sand (ϕ=45°), even at H/B=10. The displacement contour plots for H/B=3 and 8 are shown in Fig. 9 for the case of ϕ=35°. Deep anchor failure can be observed in the case of H/B=8, where the failure surface is confined within the soil around the anchor plate, and no heave is seen on the ground surface. Whereas in shallow anchor, H/B=3, a surface heave can be observed, indicating a general shear failure.

The comparison between the breakout factors of unreinforced and reinforced sand with varying embedment ratios is shown in Fig. 10. The improvement in the pullout capacity of the reinforced anchor diminishes with an increase in the H/B ratio. The improvement factor (ratio between reinforced and unreinforced pullout capacity) at H/B=1 is 48%. Whereas at H/B=10, the improvement factor is reduced to 4%. As the embedment depth increases, the unreinforced anchor's pullout capacity rises significantly due to the enormous embedment pressure acting on it. As the influence of the reinforcement reduces at higher depths, the anchor improvement factor decreases with an increase in the H/B ratio.

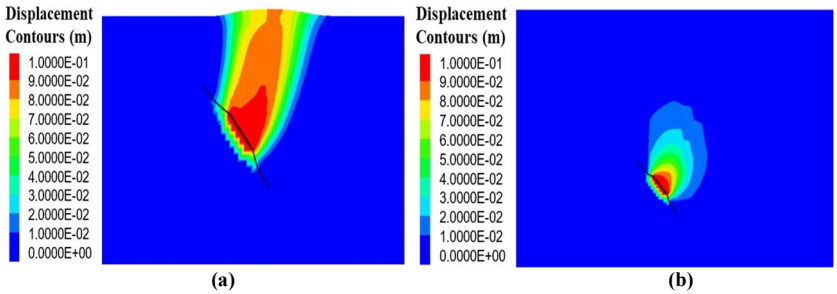

Fig. 9. Displacement contours (a) shallow anchor at H/B=3 (b) deep anchor at H/B=8.

Practical implementation to transmission tower foundations

This section uses an illustrative design example to demonstrate the use of inclined anchors for transmission tower foundations. A 36 m high transmission tower having a base width of 8 m was modeled in STAAD Pro software. The lateral wind force was applied on the tower according to ASCE guidelines [7], considering a basic wind speed of 40 m/s. The maximum uplift force in the vertical direction exerted on the tower foundation was 294 kN, produced

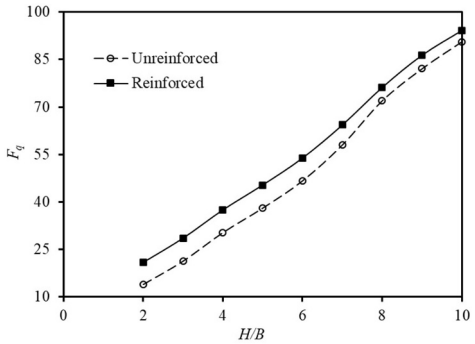

Fig. 10. Comparison of breakout factors at different embedment ratios.

by the combined effects of the self-weight of the tower and the lateral wind force. Three types of foundations were designed for the tower: pile foundation, unreinforced anchor, and reinforced anchor. The soil properties corresponding to ϕ=45° listed in Table 2 were considered in the design. The design parameters and the required depth and width of the different foundations are summarized in Table 3. The pile foundation requires a depth of 15 m to resist the uplift forces. In comparison, the inclined anchor requires a depth of 2.1 m. Moreover, the reinforced anchor requires a width of 1.5 m compared to the 2 m width needed for the unreinforced anchor. Therefore, the reinforced anchor can provide an economical solution to the transmission tower foundations.

Table 3. Summary of foundation design for transmission tower.

Pile	Unreinforced anchor	Reinforced anchors
FOS=3 Qu = W + A_s q K ′ tan(δ) :Uplift capacity of pile A_s=Embedded pile surface area q = average effective overburden pressure K' = lateral earth pressure coefficient = 0.8 [8] δ = mobilized friction angle at pile-surface interface = 2ϕ/3 D = diameter of pile = 0.3 m L = Length of pile = 15 m	FOS = 1.5 [9] Q_u =294/cos(α) α = 30° B = 2 m H = 2.1 m	FOS = 1.5 [9] Q_u =294/cos(α) α = 30° B = 1.5 m H = 2.1 m

Comparison with published experimental results

The three-dimensional numerical results are compared with experimental results reported in the literature. As there are no previously reported experimental or numerical investigations on inclined square anchors in geogrid reinforced sand, the comparison is shown only for inclined anchors in unreinforced sand. Murray and Geddes [3] conducted experiments on square inclined anchors in sand having a friction angle of 43.6°. Harvey and Burley [10] reported experiments on circular anchors inclined at 30° and 45° in sand with a friction angle of 40°. The comparison of the experimental results with the numerical simulations from the current study is shown in Fig. 11. The numerical results are slightly greater than the results reported by Murray and Geddes [3] because of the lower friction angle used in the

experiments. The slight differences in the breakout factors in Fig. 11(b) are attributed to the circular shape of the anchor plate used in the experiments.

Conclusions

A three-dimensional numerical analysis is presented in this paper investigating the pullout resistance of square inclined anchors in geogrid reinforced sand. The results indicate that the pullout capacity improves significantly in presence of the geogrid layer above the anchor plate. However, the improvement factor was found to decrease with an increase in the embedment depth of the anchor. The pullout capacity and the reinforcement's tensile force increased with the geogrid stiffness. The failure mechanism was found to be influenced by the relative density of the sand. A deep anchor failure was observed beyond H/B=8 for medium dense sand (ϕ=35°). The anchors in very dense sand (ϕ=35°) did not exhibit deep anchor failure, even at H/B=10. The application of reinforced anchors is shown for a transmission tower foundation. The results indicate that the reinforced inclined anchors can be a feasible and economical alternative to the piles and unreinforced anchors.

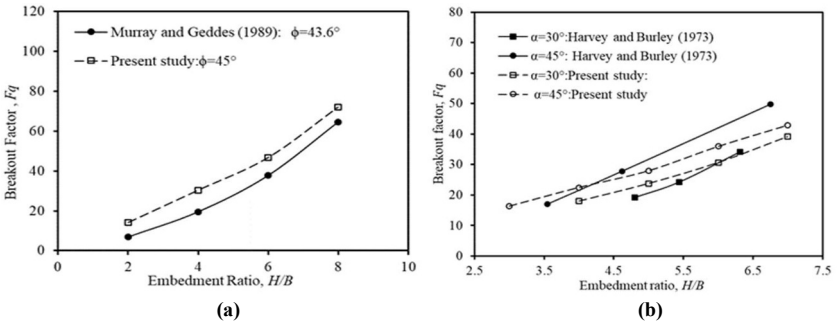

Fig. 11. Comparison of numerical results with experimental breakout factors (a) Murray and Geddes (1989): α=45° (b) Harvey and Burley (1973): α=30°, 45°; circular anchors.

References

1. M. P. Pacheco, F. A. B. Danziger, and C. P. Pinto, Eng Geol **101**, 226 (2008)
2. G. G. Meyerhof, in *8th Int. Conf. Soil Mech.* (Moscow, 1973), pp. 167–172
3. E. J. Murray and J. D. Geddes, Géotechnique **39**, 417 (1989)
4. P.-Z. Zhuang, H.-Y. Yue, X.-G. Song, H. Yang, H. Zhang, and H.-S. Yu, Canadian Geotechnical Journal **59**, 239 (2022)
5. S. Mukherjee, L. Kumar, A. K. Choudhary, and G. L. S. Babu, Geotextiles and Geomembranes **49**, 1368 (2021)
6. A. K. Choudhary, B. Pandit, and G. L. Sivakumar Babu, Geosynth Int **26**, 657 (2019)
7. ASCE (American Society of Civil Engineers), *Minimum Design Loads for Buildings and Other Structures* (2010)
8. J. E. Bowles, *Foundation Analysis and Design*, 5th ed. (McGraw-Hill Book Co., New York, 1996)
9. BUREAU OF INDLAN STANDARDS, Public Works (2006)
10. R. C. Harvey and E. Burley, Ground Engineering **65**, 48 (1973)